Quantum vibronic effects on the electronic properties of solid and molecular carbon

Arpan Kundu,[1,*] Marco Govoni,[2,1] Han Yang,[3] Michele Ceriotti,[4] Francois Gygi,[5] and Giulia Galli[1,2,3,†]

[1]*Pritzker School of Molecular Engineering, University of Chicago, Chicago, Illinois 60637, United States*

[2]*Materials Science Division and Center for Molecular Engineering, Argonne National Laboratory, Lemont, Illinois 60439, United States.*

[3]*Department of Chemistry, University of Chicago, Chicago, Illinois 60637, United States*

[4]*Laboratory of Computational Science and Modeling, IMX, Ecole Polytechnique Federale de Lausanne, 1015 Lausanne, Switzerland*

[5]*Department of Computer Science, University of California Davis, Davis, California 95616, United States*

(Dated: February 25, 2022)

Abstract

We study the effect of quantum vibronic coupling on the electronic properties of carbon allotropes, including molecules and solids, by combining path integral first principles molecular dynamics (FPMD) with a colored noise thermostat. In addition to avoiding several approximations commonly adopted in calculations of electron-phonon coupling, our approach only adds a moderate computational cost to FPMD simulations and hence it is applicable to large supercells, such as those required to describe amorphous solids. We predict the effect of electron-phonon coupling on the fundamental gap of amorphous carbon, and we show that in diamond the zero-phonon renormalization of the band gap is larger than previously reported.

Keywords: Path Integral, Electron-phonon, ZPR, Bandgap

* Corresponding author. Email: arpank@uchicago.edu

† Corresponding author. Email: gagalli@uchicago.edu

Understanding the electronic structure of materials and molecules at finite temperature is important for the prediction of the physical properties of countless systems, ranging from opto- and bio-electronic devices, to solar cells, and materials used to build quantum sensors and quantum computers. However, a general theoretical framework to study the electronic properties of molecules and solids over a wide range of temperatures, incorporating accurately nuclear quantum effects and electron-phonon interaction, is still missing.

Most theoretical studies of electron-phonon coupling have been based either on first principles molecular dynamics (FPMD) [1–4] or on perturbative calculations assuming harmonic potential energy surface (PES) [5–7]. FPMD is accurate above the Debye temperature, provided inter-atomic interactions are described at an appropriate level of density functional theory. However, for light systems, especially those containing first row elements, FPMD may not be appropriate, since nuclear quantum effects play an important role even at ambient conditions. Notable examples are liquid water [8] and ice [9, 10], many molecular crystals [11, 12], and materials and molecules composed mostly of carbon atoms, such as polymers, diamond, and graphite. In principle, perturbative [5–7] and non-perturbative stochastic [13–15] approaches, with anharmonic effects included at various levels of approximation [16, 17], may be used also below the Debye temperature, and they have been applied to several crystalline solids [13–19]. However, they are not well suited to study disordered systems, for example amorphous or glassy materials, molecular compounds and nanostructures [20].

Here we investigate the effect of electron-phonon interaction on the electronic properties of solids and molecules by accurately including quantum vibronic effects in first principles simulations. We used path integral (PI) molecular dynamics with a colored noise generalized Langevin equation (GLE), named PIGLET, to sample the appropriate quantum fluctuations of the nuclei [21]. In addition, we performed FPMD simulations with a single bead and colored noise GLE (a so-called quantum thermostat (QT) [22]). See section S2 in SI for more details. We show that the ability to perform PI simulations at a cost comparable to that of FPMD is critical to obtain accurate results for large systems.We report results for several carbon systems, including diamond, amorphous carbon (a-C), and pentamantane and we propose a simple computational protocol to predict the fundamental gap of light disordered solids including nuclear quantum effects (NQE), in an accurate and efficient manner. We predict for the first time the effect of electron-phonon coupling on the electronic properties of diamond-like a-C and we show that the zero-phonon renormalization (ZPR) of the band

gap of crystalline diamond is larger than previously reported, due to vibrational anharmonic effects. The approach proposed here permits to assess the validity of commonly used approximations in the calculation of electron-phonon interaction in molecular and condensed systems.

We start by discussing our results for diamond. At T=0, if we neglect the zero-point motion of the atoms and electron-phonon coupling, the valence band maximum (VBM) and conduction band minimum (CBM) are 3 and 6 fold degenerate, respectively. At finite T, the band edge degeneracies are broken, as shown in Fig. 1, where we report the electronic density of states (EDOS) close to the VBM and CBM of a 64 atom diamond supercell (C_{64}), obtained at 100 K from a 16-bead PIGLET simulation. The renormalized bandgap due to electron-phonon coupling may be defined in two different ways: as the energy difference between (i) the thermal average of the three eigenvalues associated to the VBM and of the six associated to the CBM (center gap) [13–15, 23, 24] or between (ii) the thermal average of the highest of the three VBM eigenvalues and of the lowest of the six CBM eigenvalues (edge gap). We show below that there is a substantial difference of $\simeq 160$ meV between the center and edge band gaps due to quantum vibronic effects; the minimum (indirect) gap of diamond corresponds to the edge gap.

We first discuss the center gap. The middle panel of Fig. 1 shows the bandgap renormalization as a function of temperature obtained with different approximations. Compared to PIGLET results, classical simulations underestimate the bandgap renormalization by more than 200 meV for T$<$ 500 K, while a QT accurately captures the NQE. The systematic error present at low T in the QT results, due to the so called zero-point energy leakage [22], leads to an extrapolated ZPR that is accurate within 30 meV. Interestingly, we found that such systematic error may be reduced to 10 meV by performing PIGLET simulations with just 2 beads, which only require twice the computational cost of a QT simulation. On the basis of this result, the NQE of all diamond supercells with more than 64 atoms were simulated using the 2-beads PIGLET protocol in both the canonical and isothermal-isobaric ensembles (labeled NVT and NPT, respectively).

The right panel of Fig. 1 compares the band gaps for a 216 atom supercell (C_{216}) with the measured indirect band gap of diamond [26] fitted using the Viña model [27]. The difference between the bandgaps obtained at constant volume and constant pressure is negligible at low temperature and it is only 30 meV at 1000 K. Therefore, we conclude that the lattice

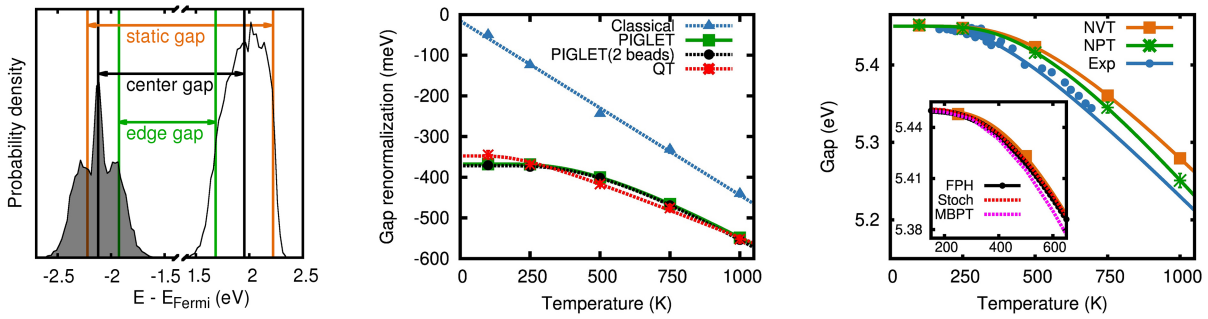

FIG. 1. (Left panel) Electronic density of states (EDOS) at the valence band maximum (VBM, shaded) and conduction band minimum (CBM) of diamond, computed with a 64 atom supercell and a 16 bead PIGLET NVT simulation at 100 K. The green, black and orange vertical lines represent the thermal average of the band edges (edge gap), the thermal average of three highest VB and six lowest CB eigenvalues (center gap), and the energy of degenerate VBM and CBM computed at the equilibrium geometry (static gap), respectively. (Middle panel) Difference between the static and center gap (gap renormalization) as a function of temperature, obtained with the same protocol used in the left panel. The symbols represent the simulation results while the lines are the Viña (linear) model fit [25] of the quantum (classical) results, respectively. Classical values are obtained with first principles molecular dynamics; results including nuclear quantum effects are obtained with PIGLET simulations (2 or more beads) and a quantum thermostat (QT). (Right panel) Center gap computed with a 216 atom supercell and 2-beads PIGLET simulations in the NVT and NPT ensembles (solid lines: Viña model fit), compared with experimental results[26, 27]. All calculated results have been offset by different amounts so that at T=0 they match the experimental bandgap extrapolated to 0 K. The inset shows the differences between results obtained using the frozen phonon harmonic approximation (FPH), a stochastic approach (Stoch) for a C_{250} supercell[15], and many-body perturbation theory (MBPT) calculations performed on a $4 \times 4 \times 4$ q-point grid[28]. Except for the NPT simulations, we used the static lattice parameter (3.568 Å) for all calculations.

thermal expansion of diamond has a negligible effect on bandgap calculations, consistent with previous studies [17, 23] carried out with an approximate treatment of anharmonicity of the PES.

We found a remarkable agreement between results obtained with the stochastic approach [15], frozen phonon harmonic results (FPH, see section S5 in the SI) and NVT simulations (see inset of Fig. 1, right panel). This indicates that the anharmonicity of the PES and

higher-order electron-phonon couplings have a negligible effect in determining the value of the center gap. In Fig. 1, we also report the results obtained by applying many-body perturbation theory (MBPT) to electron-phonon interactions and using a generalization of the method of Ref. [29] for solids [28]. The method relies on the rigid ion approximation, which assumes that the ionic Hamiltonian depends on potentials created *independently* by each nucleus. The negligible differences between MBPT values and the FPH results indicate that below $\simeq$ 500 K the rigid ion approximation is justified in the case of diamond, consistent with the conclusion of Ref. [16, 30].

Furthermore the VSCF calculations by Monserrat *et al.* yielded a ZPR (-462 meV) [17] value which is considerably larger (by about 30 %) than the corresponding harmonic (-325 meV) [31], and our FPH (-321 meV) values, as well as higher than the NVT-PIGLET result (at 100 K, -325 meV), where all calculations were performed for the same supercell (C_{250}). In contrast, by sampling the PES along each phonon mode and using the independent mode approximation, Antonius et al. [16] found that anharmonicity reduces the ZPR of the *direct* band gap of diamond by 30%. We note however that large displacements (up to 0.3 Å) along phonon modes were used in Ref. [16] which may introduce a fictitious coupling between (i) stretching and (ii) bending or torsional modes [32, 33] and hence introduce numerical artifacts.

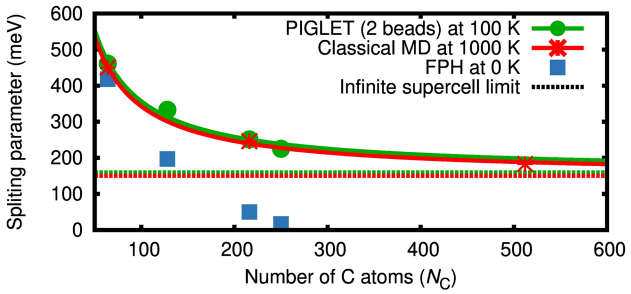

FIG. 2. Difference between the center and edge gaps of diamond (splitting parameter, which is positive definite) as a function of the number of atoms (N_C) in the supercell used in our calculations. Symbols represent the simulated data (same acronyms as in Fig.1), which were fitted (solid lines) with the function $a + b/N_C$. The dashed lines represent the extrapolated value to the infinite supercell limit.

We now turn to discussing the edge gap of diamond, defined as the difference between

the lowest non degenerate eigenvalue and the highest non degenerate eigenvalue. Previous works [14, 24] concluded that the observed splitting of degenerate bands at T close to zero is caused by the small size of the supercell adopted in DFT calculations. Zacharias and Giustino [24] claimed that the lifting of the degeneracy is caused only by the zone center phonons, and showed that their omission in the electron-phonon calculation leads to degenerate eigenvalues. In the infinite supercell size limit, the influence of zone center phonons should vanish and the splitting of degenerate bands should go to zero. We extrapolated the difference between the center and the edge gap (called here splitting parameter, which is positive definite) with respect to the number of C atoms (N_{C}) in the supercell, using the function $a + b/N_{\mathrm{C}}$, where a is a contribution independent from supercell size. Fig. 2 shows our results for the 2-beads PIGLET simulations at 100 K, classical MD simulations at 1000 K, and FPH calculations at 0 K, in a canonical ensemble using different supercell sizes. The splitting parameter converges to zero for the FPH calculations, but for the PIGLET or classical MD simulations, it converges to a non-negligible value of 160 meV. Therefore, the splitting of the band edges found here cannot be ascribed entirely to the finite size of the supercell and it represents a physical effect. Specifically, we attribute the center and edge gaps difference to anharmonic vibronic effects. We note that MD simulations sample the anharmonic PES, which is not necessarily symmetric around its minimum (see e.g, [17]) and consequently, the probability distributions along phonon modes are not Gaussians due to skewness. For example at 100 K for a C_{216} diamond supercell, we found that 234 (out of 645) phonon mode distributions deviate from a Gaussian distribution due to skewness (see section S6 in SI). This asymmetry and the consequent local dynamical disorder (see section S7 in SI) is obviously more pronounced for large amplitude oscillations and hence clearly visible at high T, e.g. 1000 K, in classical MD simulations. However, when nuclear quantum effects are considered, the asymmetry is present even at T close to zero. We emphasize that it is this asymmetry and its contribution to the ZPR that lead to a significant difference of 160 meV between the edge and central gap. In its current implementation [13–15, 24], the stochastic method, in the limit of large supercell, does not account for the center-edge splitting because it samples the probability distribution of connected harmonic oscillators without accounting for the deviations of the PES from a harmonic well. It would be interesting to explore whether the recently proposed SSCHA approximation [34, 35] is sufficiently accurate to account for the splitting observed here; we note that the SSCHA method uses

linear combinations of symmetric Gaussian functions to construct the anharmonic vibrational wave functions and hence the wave function for a non-symmetric quartic potential becomes symmetric [35], unlike the exact one.

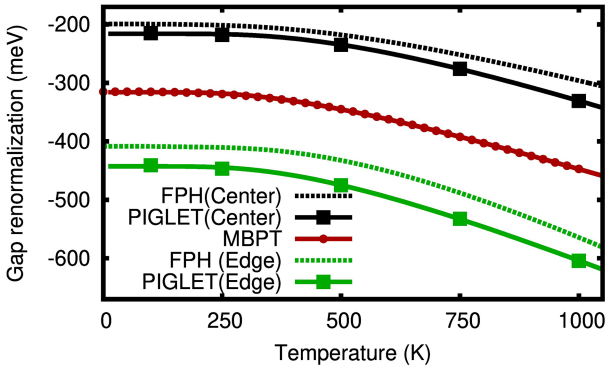

FIG. 3. Difference between the static and center and static and edge fundamental gap of a pentamantane molecule (gap renormalization), $C_{26}H_{32}$ (T_d), obtained using PIGLET simulations, and calculated with the frozen phonon harmonic approach (FPH) and many-body perturbation theory (MBPT). The renormalization of both the center and edge gap is reported in the case of FPH and PIGLET calculations. By construction, the difference between center and edge gaps is zero within MBPT.

In order to explore whether a difference between center and edge gaps is observed also for carbon nanostructures, we studied the electronic properties of the pentamantane molecule. Fig. 3 shows the results from PIGLET simulations and FPH calculations (See also Fig. S8 in the SI). The ZPR of the center gap (FPH: -200 meV, PIGLET: -220 meV) is consistent with previous estimates at the PBE level of theory (-210 meV) [36]. However, the ZPR of the edge gap (FPH: -405 meV, PIGLET: -445 meV) is twice as large and certainly this value is not affected by the size of the supercell, since we are considering an isolated molecule. The presence of the splitting observed here was also reported in previous *ab-initio* studies of small diamondoids [37, 38], and Gali *et al.* suggested that the fine structure of the diamondoid photoemission spectra can only be explained by considering such a splitting [38]. We suggest that, as in the case of crystalline diamond, the edge gap is the most appropriate definition for the single particle gap in the case of the pentamantane molecule, since by definition the measurement of a gap by photoemission is a measure of the energy difference between the highest occupied and the lowest unoccupied single particle orbitals. Note that, unlike

diamond, the splitting observed for pentamantane does not only stem from anharmonic effects because FPH calculations also yield a sizeable splitting. The comparison of FPH and PIGLET results for pentamantane shows that even at high temperatures, the combined contribution of (i) anharmonicity of the PES and (ii) higher order electron-phonon coupling does not amount to more than 10% of the total electron-phonon renormalizations of the edge gap.

In Fig. 3, we also show the finite temperature electron-phonon renormalizations calculated using the MBPT approach as implemented in the WEST code[39] and presented in Ref. [29]. In addition to the harmonic approximation, the calculations of Ref. [29] used the rigid-ion approximation, finding a result for the center gap which differs by 100 meV from that obtained with the FPH approach. This difference indicates that the rigid ion approximation is not sufficiently accurate for molecular systems, e.g., isolated molecules, and, we expect, for molecular crystals as well. For diatomic molecules, similar observations were previously reported by Gonze *et al* [40].

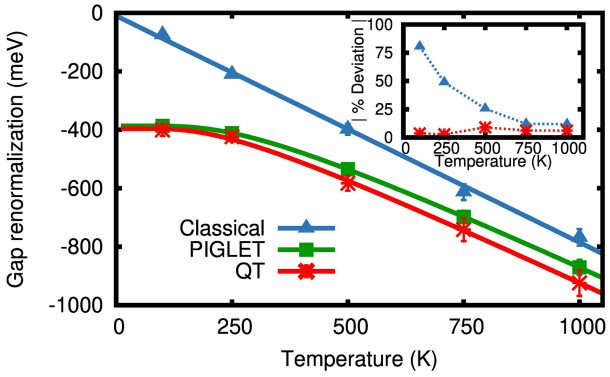

FIG. 4. Difference between the minimum static and center gap (gap renormalization) computed for amorphous-C obtained using different methods to treat nuclear quantum effects (acronyms as in Fig.1). We carried out NVT simulations for an a-C sample with density of 3.25 g/cm^3, from ref. [41]. The inset shows the absolute percentage deviation of (i) classical molecular dynamics (MD) and (ii) MD with a quantum thermostat from PIGLET simulations.

As in the case of the diamond crystal, we compared QT and PIGLET gap renormalization results for pentamantane over a wide range of temperatures and found excellent agreement (see Fig S9), indicating that the use of a QT is adequate for MD simulation studies of single particle gaps of molecular systems, and it is expected to be particularly valuable for larger

nanostructures and when costly functionals such as meta-GGA or hybrid functionals are adopted.

Finally, we present results for a diamond-like amorphous carbon (DLC), which is an example of a disordered system, where both localized and extended electronic states are present and where there are no degenerate electronic states. In addition to classical MD, we used PIGLET as well as MD with a QT to investigate the effects of NQE on the renormalization of the minimum gap, and the results are shown in Fig 4 for a 216 atom sample.

For T $<$ 250 K, neglecting NQE severely affects the bandgap renormalization, which is underestimated by more than 50% in the classical MD simulations, relative to the PIGLET results. As T is increased, as expected, the classical description becomes increasingly more accurate, with only $\sim$10% deviations at 1000 K. The bandgap predictions from classical MD are, therefore, not accurate for most applications with a working temperature range of 250 - 350 K. Interestingly, we find that in spite of the presence of some localized states in the system, which are expected to be less sensitive to electron-phonon renormalization than extended states [28], the overall ZPR of the band gap of a-C is substantial ($\simeq$ 400 meV at low T), amounting to about two third of that found for crystalline diamond. Finally, we note the excellent agreement between QT and PIGLET results below 500 K, confirming that MD simulations with either a QT or 2 beads-PIGLET represent a promising, pragmatic choice that does not add a substantial computational overhead to classical FPMD (see section S3). This result is particularly important for the modelling of amorphous systems, where it is usually necessary to average results over multiple configurations obtained from separate annealing processes; in addition, large samples with several hundreds of atoms are often required to represent the medium range order in these systems; hence, performing PIGLET simulations with a large number of beads may not be computationally feasible.

In summary, we investigated the effect of quantum vibronic coupling on the electronic properties of light molecules and solids, including ordered and disordered systems, by coupling FPMD with a generalized quantum thermostat which accounts for anharmonic effects in the ionic potential energy surface. Our approach avoids all the approximations commonly made in calculations of electron-phonon coupling, including the rigid-ion and the harmonic approximation. Importantly, it is an efficient approach, which only adds a moderate computational cost to FPMD simulations and hence it is applicable to large supercells, such as those required to describe amorphous solids.

We found that in molecular and solid carbon based materials, nuclear quantum effects significantly alter the electron-phonon band gap renormalizations at temperatures below 500 K. Our calculations showed that in diamond, even at temperatures close to zero, the degeneracy of the band edges is lifted due to vibrational, anharmonic effects, and the resulting zero phonon renormalization (ZPR) of the band gap due to electron-phonon interaction is $\sim$160 meV, larger than previously reported at the same level of theory. With continuing improvement in the resolution of photoemission experiments [42], we believe our predictions are amenable to experimental validation. The ZPR is substantial also for diamond-like a-C, albeit about 30% smaller than in crystalline diamond. Similar to the solid phases, we also observed a large ZPR (445 meV) for the pentamantane molecule.

Finally, our simulations allowed us to asses the validity of common approximations used in the literature to study electron-phonon coupling. We showed that the rigid-ion approximation, widely applied in MBPT based methods, though adequate for extended solids such as diamond at low temperatures (< 500 K), is severely deficient for molecular systems (e.g., Pentamantane). We found that stochastic non-perturbative methods are promising approaches; however, in their current implementation they cannot account for the splitting of degenerate orbitals originating from the dynamical disorder found in diamond, due to its anharmonic potential energy surface. Work is in progress to apply the computational protocol to heterogeneous and disordered systems where both localized and delocalized electronic states are present, for example point defects in diamond and amorphous and glassy carbon with different densities.

ACKNOWLEDGMENTS

We thank S. Kundu and B. Monserrat for useful discussions. We thank G. Cicero and F. Risplendi for providing the coordinates of diamond like amorphous carbon simulated from first principles. This work was supported by MICCoM, as part of the Computational Materials Sciences Program funded by the U.S. Department of Energy. This research used

resources of the University of Chicago Research Computing Center.

[1] D. Marx and J. Hutter, *Ab Initio Molecular Dynamics: Basic Theory and Advanced Methods* (Cambridge University Press, 2009).

[2] T. R. S. Prasanna, Relation between ab initio molecular dynamics and electron-phonon interaction formalisms (2009), arXiv:0902.0719.

[3] G. Galli, R. M. Martin, R. Car, and M. Parrinello, Phys. Rev. Lett. **62**, 555 (1989).

[4] K. Prasai, P. Biswas, and D. A. Drabold, Semicond Sci Technol **31**, 073002 (2016).

[5] M. Cardona, Solid State Commun **133**, 3 (2005).

[6] F. Giustino, Rev. Mod. Phys. **89**, 015003 (2017).

[7] B. Monserrat, J. Phys. Condens. Matter **30**, 083001 (2018).

[8] M. Ceriotti, W. Fang, P. G. Kusalik, R. H. McKenzie, A. Michaelides, M. A. Morales, and T. E. Markland, Chem. Rev. **116**, 7529 (2016).

[9] B. Pamuk, J. M. Soler, R. Ramírez, C. P. Herrero, P. W. Stephens, P. B. Allen, and M.-V. Fernández-Serra, Phys. Rev. Lett. **108**, 193003 (2012).

[10] S. J. Buxton, D. Quigley, and S. Habershon, J. Chem. Phys. **151**, 144503 (2019).

[11] M. Rossi, P. Gasparotto, and M. Ceriotti, Phys. Rev. Lett. **117**, 115702 (2016).

[12] C. Cazorla and J. Boronat, Rev. Mod. Phys. **89**, 035003 (2017).

[13] M. Zacharias, C. E. Patrick, and F. Giustino, Phys. Rev. Lett. **115**, 177401 (2015).

[14] M. Zacharias and F. Giustino, Phys. Rev. B **94**, 075125 (2016).

[15] F. Karsai, M. Engel, E. Flage-Larsen, and G. Kresse, New J. Phys. **20**, 123008 (2018).

[16] G. Antonius, S. Poncé, E. Lantagne-Hurtubise, G. Auclair, X. Gonze, and M. Côté, Phys. Rev. B **92**, 085137 (2015).

[17] B. Monserrat, N. D. Drummond, and R. J. Needs, Phys. Rev. B **87**, 144302 (2013).

[18] F. Giustino, S. G. Louie, and M. L. Cohen, Phys. Rev. Lett. **105**, 265501 (2010).

[19] E. Cannuccia and A. Marini, Phys. Rev. Lett. **107**, 255501 (2011).

[20] V. Kapil, E. Engel, M. Rossi, and M. Ceriotti, J. Chem. Theory Comput. **15**, 5845 (2019).

[21] M. Ceriotti and D. E. Manolopoulos, Phys. Rev. Lett. **109**, 100604 (2012).

[22] M. Ceriotti, G. Bussi, and M. Parrinello, Phys. Rev. Lett. **103**, 030603 (2009).

[23] R. Ramírez, C. P. Herrero, and E. R. Hernández, Phys. Rev. B **73**, 245202 (2006).

[24] M. Zacharias and F. Giustino, Phys. Rev. Research **2**, 013357 (2020).

[25] L. Viña, S. Logothetidis, and M. Cardona, Phys. Rev. B **30**, 1979 (1984).

[26] C. D. Clark, P. J. Dean, P. V. Harris, and W. C. Price, Proc. Royal Soc. A Math. Phys. Sci. **277**, 312 (1964).

[27] K. P. O'Donnell and X. Chen, Appl. Phys. Lett **58**, 2924 (1991).

[28] H. Yang, M. Govoni, A. Kundu, and G. Galli, Combined first-principles calculations of electron-electron and electron-phonon self-energies in condensed systems (2021), arXiv:2106.10373.

[29] R. L. McAvoy, M. Govoni, and G. Galli, J. Chem. Theory Comput. **14**, 6269 (2018).

[30] A. Edström, J. Chico, A. Jakobsson, A. Bergman, and J. Rusz, Phys. Rev. B **90**, 014402 (2014).

[31] B. Monserrat, Phys. Rev. B **93**, 014302 (2016).

[32] G. Piccini and J. Sauer, J. Chem. Theory Comput. **9**, 5038 (2013).

[33] G. Piccini and J. Sauer, J. Chem. Theory Comput. **10**, 2479 (2014).

[34] I. Errea, M. Calandra, and F. Mauri, Phys. Rev. B **89**, 064302 (2014).

[35] L. Monacelli and F. Mauri, Time-dependent self consistent harmonic approximation: Anharmonic nuclear quantum dynamics and time correlation functions (2020), arXiv:2011.14986.

[36] P. García-Risueño, P. Han, and G. Bester, Frozen-phonon method for state anticrossing situations and its application to zero-point motion effects in diamondoids (2019), arXiv:1904.05385.

[37] C. E. Patrick and F. Giustino, Nat. Commun **4**, 2006 (2013).

[38] A. Gali, T. Demján, M. Vörös, G. Thiering, E. Cannuccia, and A. Marini, Nat. Commun **7**, 11327 (2016).

[39] M. Govoni and G. Galli, J. Chem. Theory Comput. **11**, 2680 (2015).

[40] X. Gonze, P. Boulanger, and M. Côté, Annalen der Physik **523**, 168 (2011), https://onlinelibrary.wiley.com/doi/pdf/10.1002/andp.201000100.

[41] F. Risplendi, M. Bernardi, G. Cicero, and J. C. Grossman, Appl. Phys. Lett **105**, 043903 (2014).

[42] H. Iwasawa, H. Takita, K. Goto, W. Mansuer, T. Miyashita, E. F. Schwier, A. Ino, K. Shimada, and Y. Aiura, Sci. Rep. **8**, 17431 (2018).